Multicarrier DS-CDMA System Under Fast Rician Fading and Partial-Time Partial-Band Jamming

Kanke Wu, Pamela C. Cosman, *Fellow, IEEE*, and Laurence B. Milstein, *Fellow, IEEE*

***Abstract*— The impact of joint partial-time, partial-band jamming on a multicarrier (MC) asynchronous direct-sequence code-division multiple access (DS-CDMA) system in a fast fading environment is studied in conjunction with two different subcarrier combining and decoding schemes. An easy-to-evaluate upper bound using the Chernoff bound is provided and compared to simulation results. Simulation results suggest that for soft-decision decoding systems, under Rayleigh fading, full-time, full-band jamming is most effective. In contrast to the Rayleigh case, when a sufficiently strong line-of-sight component exists in the channel, the jammer's optimal strategy of attacking in time or frequency depends on the strength and the type of error correction that the system is deploying for that dimension. For hard-decision decoding systems, in Rayleigh fading, partial-band jamming is recommended. For the coding strategies examined, in Rician fading, the jammer should switch from full-time, partial-band jamming to a strategy that jams a higher percentage of the more heavily protected dimension as the jamming power increases. Furthermore, for AWGN channels, the results from the system show that the jammer should always jam a higher percentage of the more heavily protected dimension.**

***Index Terms*— Code division multiaccess, multipath channels, rician channels, jamming.**

I. Introduction

DIFFERENT realizations of multitone direct-sequence code-division multiple access (DS-CDMA) and multicarrier (MC) DS-CDMA systems have been proposed and their performances have been analyzed in many publications [1]–[8]. It is well-known that DS-CDMA systems are vulnerable to partial-time jamming [9], [10], and in [11], [12] it can be seen that, depending on the design, multicarrier systems can be vulnerable to partial-band jamming. In this paper, we focus on the performance of the MC-DS-CDMA system described in [1] under joint partial-time, partial-band jamming.

The performance of DS-CDMA systems undergoing a jamming attack has been studied extensively for the single carrier case. In [9], [13], [14] the performance of coded and uncoded single carrier DS-CDMA systems under fading and partial-time jamming was studied. A RAKE receiver was employed to exploit path diversity. The result can be adapted to MC-DS-CDMA systems with maximal-ratio combining. In [15]–[17] the performance of MC CDMA systems under full-time, partial-band jamming was studied. And in [2], the performance of MC-DS-CDMA under full-time, partial-band jamming was studied for both narrowband Gaussian noise and continuous-wave tone interference.

However, there are not many studies on the performance of MC-DS-CDMA systems under joint partial-time, partial-band jamming. In [8], the performance of uncoded MC-DS-CDMA under optimized joint partial-time, partial-band jamming was studied for both AWGN channels and Rayleigh fading. There it was assumed that the background noise is negligible compared to the jammer. As a result, full-band jamming is always optimal when maximal-ratio combining is used, since any unjammed subcarrier will dominate the test statistics.

There have been many studies on intelligent jamming in the literature. In [18], the authors looked into intelligent jamming on wireless networks by using knowledge of protocol, and exploiting crucial timing and control packets to degrade the performance of the system. Similarly, in [11], [19] the authors also used knowledge of the crucial timing in the system to optimize the jammer's power allocation between spoofing and jamming to limit the overall system performance. In [20], the authors considered the impact of a disguised jammer on DS-CDMA systems, where the disguised jammer uses a fake signal with the same spreading code and constellation as the system. All of the above approaches to jamming strategy optimization require some level of knowledge about the system. While knowledge, such as system timing, can be relatively easy to obtain, other information, such as the spreading code used in the system, is usually not available to the jammer. When the jammer has only limited information on the system structure, a Gaussian noise signal is usually used as a jamming signal model during the data transmission period [9]. The optimization of jamming parameters has been studied for a DS-CDMA system with partial-time jamming [9] and for a multi-carrier system with partial-band jamming [11]. Although [2] provided analysis on the performance of a MC-DS-CDMA system under partial-band jamming, there was no discussion on how the result can be used in optimizing the jamming strategy. Other literature, such as [21]–[24], also focus on the system performance of multicarrier DS-CDMA systems under various jamming models without providing

Manuscript received May 10, 2018; revised October 26, 2018, March 1, 2019, and May 30, 2019; accepted June 21, 2019. Date of publication July 3, 2019; date of current version October 16, 2019. This research was supported by the Army Research Office under Grant W911NF-14-1-0340. The associate editor coordinating the review of this paper and approving it for publication was Y.-W.P. Hong. *(corresponding author: Kanke Wu.)*

The authors are with the Department of Electrical and Computer Engineering, University of California at San Diego, San Diego, CA 92093-0407 USA (e-mail: k6wu@ucsd.edu; pcosman@ucsd.edu; lmilstein@ucsd.edu).

Color versions of one or more of the figures in this article are available online at http://ieeexplore.ieee.org.

Digital Object Identifier 10.1109/TCOMM.2019.2926729

insights on how the results can be used by the jammer to optimize its jamming strategy, or include joint partial-time, partial-band jamming as one of the jamming models.

The motivation for the research is our interest in determining both how an intelligent adversary can most effectively jam the system, and how much degradation in system performance the adversary can cause. The adversary considered in our study uses joint partial-time, partial-band jamming signals and has a limited average power. It aims to disrupt communication between the transmitter and receiver by intentionally transmitting interference signals to decrease the signal-to-interference-and-noise ratio at the receiver. Since partial-time jamming by itself, and partial-band jamming by itself, are special cases of joint partial-time, partial-band jamming, the joint jamming attack has to be at least as effective as either of the two separate attacks.

We study system performance in a fast Rician fading environment in the presence of joint partial-time, partial-band Gaussian jamming. We discuss jamming parameter selection based on an analytical upper bound. Unlike [2], where partial-band jamming is considered, we do not assume knowledge of which bands are being jammed. Compared to [8], we consider a coded system without ignoring thermal noise. Also, we extend the results in both papers to a more generalized channel model.

The system described in [1] and relevant test statistics are reviewed in Sections II-A and II-C. The jammer model is defined in Section II-B. The performance of the system under joint partial-time, partial-band jamming is analyzed. Results for soft-decision decoding can be found in Section III-A and IV. Results for hard-decision decoding can be found in Section III-B. Numerical results and discussion are provided in Section V, and conclusions are provided in Section VI.

II. System Model and Analysis

A. Transmitter and Receiver

The model we use is an uplink single cell MC-DS-CDMA system with a central controller. A total of Q users share N subcarriers. The system is adapted from the design in [1]. The transmitter and receiver are shown in Figs. 1 and 2, respectively. All Q users occupy the entire frequency band at the same time, and transmit with power P^s on each subcarrier. Pseudo-noise (PN) sequences are used as signature sequences, and different transmitting rates can be achieved by assigning multiple sequences to the same user. It is assumed that the sequences assigned to the same user are orthogonal to one another. QPSK modulation is used on each subcarrier.

The data bit sequence $\underline{\mathbf{d}}_q$ is first encoded with rate–$1/M$ forward error correction (FEC) to produce the FEC-encoded codeword symbol sequence $\underline{\mathbf{c}}_q$. Sequence $\underline{\mathbf{c}}_q$ is then interleaved and mapped to $n_q M N_{bits}$ streams, with n_q being a positive integer representing the number of spreading codes user q needs, and N_{bits} being the number of information bits the system can transmit over one time slot with one stream. Each stream is then repeated $2R$ times and mapped onto one of the $2N$ in-phase and quadrature output components, where

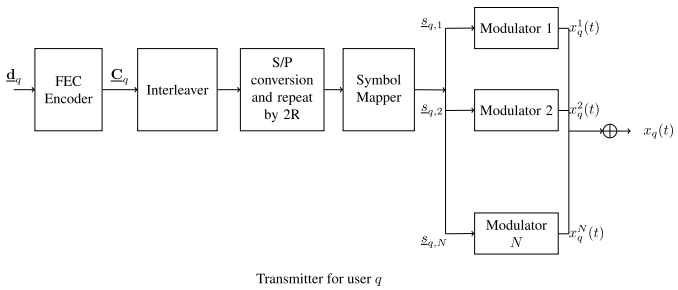

Fig. 1. Transmitter diagram for user q.

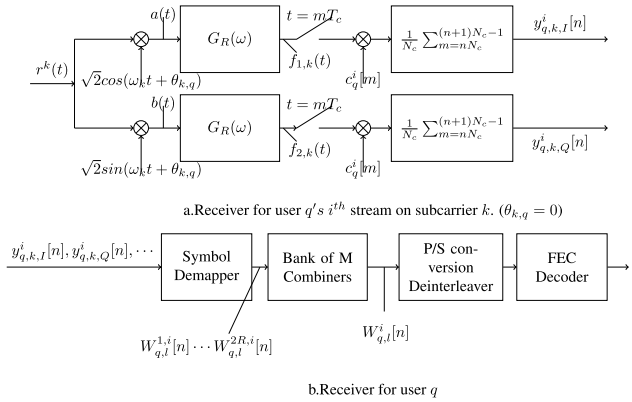

Fig. 2. Receiver for user q on subcarrier k.

$N = N_{bits} M R$ is the total number of subcarriers in the system, each with a bandwidth of BW_0.

The channel is assumed to experience frequency-selective Rician fading over the system bandwidth BW. The power from the direct path is $\bar{\alpha}_D^2$, the power from indirect paths is $\bar{\alpha}_R^2$, and the K-factor for the channel is $K_{fac} \triangleq \bar{\alpha}_D^2 / \bar{\alpha}_R^2$. The subcarrier bandwidth and subcarrier number are chosen to guarantee that each subcarrier undergoes flat fading. The background thermal noise with a double-sided power spectral density of $\eta_0/2$ is added to the received signal.

The mapping between FEC-coded symbols and subcarriers is such that the in-phase and quadrature components of any subcarrier are modulated by different FEC-coded symbols, and the frequency separation between the replicas of any coded symbol is maximized. It is easy to see that one such mapping (assuming $n_q = 1$) is

$$\begin{aligned} s_{q,k,I}^{(1)}[n] &= c_q^{(n-1)MN_{bits}+1+\{k-1, mod\ MN_{bits}\}}, \ k = 1, \cdots, N. \\ s_{q,k,Q}^{(1)}[n] &= c_q^{(n-1)MN_{bits}+1+\{k-1+\lfloor MN_{bits}/2 \rfloor, mod\ MN_{bits}\}}, \\ & \qquad k = 1, \cdots, N. \end{aligned} \tag{1}$$

A square-root-raised-cosine wave shaping filter with roll-off factor $\beta \in [0, 1]$ is used to limit signal bandwidth and avoid inter symbol interference (ISI). After modulating the assigned subcarriers, the signal $x_q^k(t)$ is formed, and finally, the sum of all the $x_q^k(t)$ is the transmitted signal for user q.

The receiver structure for user $q's$ i^{th} stream on subcarrier k is given in Fig. 2. A matched filter receiver is used for each of the streams, and the filtered signal is sampled and

despread to produce sequences $y^i_{q,k,I}[n]$ and $y^i_{q,k,Q}[n]$, where n is a generic sample index and takes on integer values. A reverse operation of the mapping described in (1) is carried out to produce M partitions of $2R$ terms, which are referred to by $W^{j,i}_{q,l}[n]$. Each partition is maximal-ratio or majority-voting combined to produce the test statistic corresponding to each of the M coded symbols, denoted by $W^i_{q,l}[n]$ and $D^i_{q,l}[n]$ respectively. These symbols are then deinterleaved and put through a Viterbi decoder to produce the decoded data.

B. Jammer

The jammer is on for ρ_T percent of the time, jamming ρ_F percent of the subcarriers when it is on. The jamming waveform used is narrowband Gaussian noise. The power spectral density of the narrowband interference (NBI) is given by

$$S_J(f) = \begin{cases} \dfrac{\eta_J}{2}, & \dfrac{2f_i - BW_0}{2} \le |f| \le \dfrac{2f_i + BW_0}{2}, i = 1, \cdots, N_J. \\ 0, & otherwise. \end{cases} \tag{2}$$

The partial-time jamming ratio is defined as $0 < \rho_T \le 1$, and the partial-band jamming ratio is defined as $\rho_F = N_J/N$, where $N_J = 1, 2, \ldots, N$ is the number of subcarriers being jammed. Let $\eta_{J0}/2$ be the two-sided power spectral density of a full-band, full-time jammer ($\rho_T = 1,\ \rho_F = 1$). For $\rho_T \ne 1,\ \rho_F \ne 1$, the two-sided power spectral density for a jammed subcarrier when the jammer is on is given by

$$\frac{\eta_J}{2} = \frac{\eta_{J0}}{2\rho_T \rho_F}. \tag{3}$$

C. Test Statistics at Receiver

Test statistics at the receiver can be derived by modifying results given in [1] and [2]. Let $H(k,q)$ be the complex envelope of the channel at subcarrier k between user q and the central controller, and let $\alpha(k,q) = |H(k,q)|$. Let N_c be the spreading factor of the system.

To calculate the coded error rate, one must first derive the test statistics of $W^{j,i}_{q,l}[n]$ and $W^i_{q,l}[n]$. Since the $W^{j,i}_{q,l}[n]$'s are just rearranged versions of $y^i_{q,k,*}[n]$'s, they have the same statistics. It was shown in [2] that the expression for $y^i_{q,k,*}[n]$'s has four components: signal component $S^i_{q,k,*}[n]$, multiple-access-interference (MAI) component $I^i_{q,k,*}[n]$, noise component $N^i_{q,k,*}[n]$, and jamming component $J^i_{q,k,*}[n]$ ($*$ is cos for the output of the inphase component and is sin for the quadrature component).

The signal component $S^i_{q,k,*}[n]$ is given by

$$S^i_{q,k,*}[n] = \sqrt{P^s}|H(k,q)|s^i_{q,k,*}[n]. \tag{4}$$

The transmitted bit energy for user q is

$$E_b = \sum_{k=1}^{2MR} \sum_{j=0}^{N_c-1} P^s = 2MRN_cP^s. \tag{5}$$

The MAI component $I^i_{q,k,*}[n]$ is asymptotically zero-mean Gaussian in the number of users Q. Its variance can be approximated as

$$\mathbb{E}[\left(I^i_{q,k,cos}[n]\right)^2] = Var[I^i_{q,k,cos}[n]] = Var[I^i_{q,k,sin}[n]] \approx \sum_{r \ne q} P^s \bar{\alpha}^2_r \frac{n_r}{N_c}(1 - \frac{\beta}{4}). \tag{6}$$

as shown in [25]. Here, $\bar{\alpha}_r$ is the average channel gain between user r and the central controller. Also, $\mathbb{E}[I^i_{q,k,cos}[n] I^j_{q,k,sin}[m]] = 0,\ \forall m,n,i,j$; $\mathbb{E}[I^i_{q,k,cos}[n] I^j_{q,k,cos}[m]] = 0,\ \forall m \ne n,\ \forall i,j$; and finally $\mathbb{E}[I^i_{q,k,cos}[n] I^j_{q,k,cos}[n]] = 0,\ \forall i \ne j$.

The noise component $N^i_{q,k,*}[n]$ does not depend on the sampling time or the frequency position and is the same for all users. They are i.i.d Gaussian with zero mean and variance $\sigma_0^2 = \eta_0/(2N_c)$.

Finally, the jamming component $J^i_{q,k,*}[n]$ only depends on the jammer state. It is the same for all users. Let J^{cos}_k and J^{sin}_k be the jammer components on the in-phase and quadrature channels of subcarrier k. $J^{cos/sin}_k[n]$ is a zero mean, conditionally Gaussian random variable, with variance

$$Var[J^{cos/sin}_k[n]] = \frac{1}{N_c^2} \sum_{l=nN_c}^{(n+1)N_c-1} \sigma^2_{J,*}[l], \tag{7}$$

where $\sigma^2_{J,*} = (\alpha^2_J \eta_J)/2$ when the jammer is present, and $\sigma^2_{J,*} = 0$ otherwise.

Further, it can be shown that, conditioned on the channel gain between the desired user and the central controller, the distributions of $y^i_{q,k,*}[n]$'s (and hence $W^{j,i}_q[n]$'s) are asymptotically Gaussian in the number of users Q, and they are conditionally independent of each other.

1) Maximal Ratio Combining: A maximal-ratio combiner with operation given by $W^i_{q,l}[n] = \sum_{j=1}^{2R} g^j_q[n] W^{j,i}_{q,l}[n]$, and perfect channel state information, is assumed. The coefficient $g^j_q[n]$ is

$$g^j_q[n] = \frac{\mathbb{E}\{W^{j,i}_{q,l}[n] | \alpha(\nu(l,j),q)\}}{Var\{W^{j,i}_{q,l}[n] | \alpha(\nu(l,j),q)\}} = \frac{\alpha_{q,\nu(l,j)}}{\sigma^2_{\nu(l,j)}}, \tag{8}$$

where $\nu(l,j)$ maps the j^{th} copy of the l^{th} symbol to the corresponding subcarrier. Finally,

$$W^{j,i}_{q,l}[n] = \begin{cases} y^i_{q,\nu(l,j),cos}[\lceil \dfrac{n}{M} \rceil], & for\ j = 1, \cdots, R \\ y^i_{q,\nu(l,j),sin}[\lceil \dfrac{n}{M} \rceil], & for\ j = R+1, \cdots, 2R \end{cases} \tag{9}$$

specifies the mapping between $W^{j,i}_{q,l}$'s and $y_{q,k,*}$'s. We can conclude that $W^i_{q,l}[n]$ is a sum of conditionally, uncorrelated, jointly Gaussian random variables:

$$W^i_{q,l}[n]|_{\gamma_i} \underset{Q \to \infty}{\to} N(\pm\sqrt{P^s}\gamma_i, \gamma_i), \tag{10}$$

where

$$\gamma_i \triangleq \sum_{j=1}^{2R} \frac{\alpha^2_{q,\nu(i,j)}}{\sigma^2_{\nu(l,j)}}. \tag{11}$$

The sign of the mean depends on the transmitted bit, and $\sigma_{\nu(i,j)}$ is the corresponding background noise standard deviation.

2) Majority-Voting Combining: When a majority-voting combiner is used, a hard decision is made based on each of the $2R$ received diversity components, $W_{q,l}^{j,i}[n]$, by comparing to a threshold R. This creates the decision variables $D_{q,l}^{j,i}[n] \in \{0,1\}$. Majority voting combining is then used to decide the final decision $D_{q,l}^{i}[n]$, so that

$$D_{q,l}^{i}[n] = \begin{cases} 0, & if \ \sum_{j=1}^{2R} D_{q,l}^{j,i} < R. \\ 1, & if \ \sum_{j=1}^{2R} D_{q,l}^{j,i} > R. \\ pick\ at\ random, & if \ \sum_{j=1}^{2R} D_{q,l}^{j,i} = R. \end{cases} \quad (12)$$

III. Coded Performance in Fast Fading

Throughout this section, we use a rate–$1/M$ convolutional code, which was chosen for its tractability. We also assume a fast Rician fading environment. With sufficient interleaving, the vector of M deinterleaved, combined receiver outputs at time index l is given by $Y_l = [Y_{1,l}, Y_{2,l}, \ldots, Y_{M,l}]$, and the components of Y_l are independent, conditionally, jointly Gaussian random variables, conditioned on the channel gains between the desired user and the central controller. The components of Y_l come from deinterleaving the W_q^i's or D_q^i's.

A. Soft Decision Decoding

In this section, we use the maximal-ratio combiner described in Section II-C.1. We start our examination of the performance of the system by considering a partial-time jammer that jams each symbol independently with probability ρ_T. The result derived based on this partial-time jammer mode can be extended to the case where the jammer jams a continuous segment that constitutes ρ_T percent of an entire transmitted codeword, since the average performance of the system under the burst jamming mode is almost identical to the performance under the first jamming mode [26].

When the jammer jams each symbol independently with probability ρ_T, we can bound the average error probability of the jammed system by first averaging over the partial-time jamming, and then averaging over the partial-band jamming. The Chernoff bound in conjunction with the union bound is used in bounding the error probability.

Without loss of generality, assume we are decoding the 1^{st} stream of user q. Let $\mu_l^{(r)}$ be the branch metric of the rth path through the decoder trellis at time index l (conditioned on the channel gains), and $b_{i,l}^{(r)}$ be the ith coded symbol of the rth trellis path at time index l for the desired user. Let γ be a vector of SNRs for each of the coded symbols. Conditioned on γ, the expression for $\mu_l^{(r)}$ takes on the form of the well-known inner-product branch metric for the AWGN channel. The r^{th} path metric is defined as [10]:

$$U^{(r)} = \sum_{l=1}^{B} \mu_l^{(r)} = \sum_{l=1}^{B} \sum_{i=1}^{M} \left(Y_{i,l} \cdot b_{i,l}^{(r)} \right), \quad (13)$$

where $[b_{1,l}^{(r)}, b_{2,l}^{(r)}, \cdots, b_{M,l}^{(r)}]$ represents the codeword that corresponds to the branch of the r^{th} path at time index l. B is the truncated depth in the trellis.

For a linear binary convolutional code, the coded performance can be evaluated by assuming the all-zero sequence ($r = 0$) is transmitted and some competing path is selected by the decoder ($r = 1$). The conditional probability of selecting a competing path over the all-zeros path is

$$P(U^{(1)} - U^{(0)} \geq 0) = P\left(\sum_{l=1}^{B} \sum_{i=1}^{M} Y_{i,l} \left[b_{i,l}^{(1)} - b_{i,l}^{(0)} \right] \geq 0 \right). \quad (14)$$

The term in the square brackets vanishes except for the locations where a code symbol error occurs. Let d_i be the number of code symbol errors. If each of the coded symbols is jammed independently of each other in time, and with probability equal to the partial-time jamming ratio ρ_T, the average probability of selecting $r = 1$ when $r = 0$ was transmitted, given there are d_i symbol differences between $r = 1$ and $r = 0$, can be calculated as

$$\overline{P\left(U^{(1)} - U^{(0)} \geq 0 \middle| \, d_i\right)} = \sum_{j=0}^{d_i} \binom{d_i}{j} \rho_T^j (1-\rho_T)^{d_i - j} P\left(U^{(1)} - U^{(0)} \geq 0 \middle| \, d_i, j\right), \quad (15)$$

where $P\left(U^{(1)} - U^{(0)} \geq 0 \middle| \, d_i, j\right)$ means selecting path $r = 1$ when path $r = 0$ was transmitted, given there are d_i errors in path-1 and that j of those error symbols were jammed.

We now compute $P\left(U^{(1)} - U^{(0)} \geq 0 \middle| \, d_i, j\right) = \mathbb{E}_\alpha \left[P\left(U^{(1)} - U^{(0)} \geq 0 \middle| \, d_i, j, \alpha\right) \right]$. Let $\mathcal{E}$ be the set of (i,l) where $Y_{i,l}$ represents an error. Let $\mathcal{J}$ be the set of (i,l) where $Y_{i,l}$ represents a jammed code symbol received in error. By definition, their cardinalities satisfy $|\mathcal{E}| = d_i$, $|\mathcal{J}| = j$. Also define

$$G_{k,N_J} \triangleq \frac{\binom{N_J}{k}\binom{N-N_J}{2R-k}}{\binom{N}{2R}}. \quad (16)$$

Then

$$P\left(U^{(1)} - U^{(0)} \geq 0 \middle| \, d_i, j\right) = \mathbb{E}_\alpha \left[P\left(\sum_{(i,l)\in\mathcal{E}} Y_{i,l} \leq 0 \middle| \, d_i, j, \alpha \right) \right] \quad (17)$$

$$< \mathbb{E}_\alpha \left\{ \min_{\rho>0} \mathbb{E}_{Y_{i,l}|\alpha} \left[e^{-\rho\left(\sum_{(i,l)\in\mathcal{E}} Y_{i,l}\right)} \middle| \, d_i, j \right] \right\} \quad (18)$$

$$\leq \mathbb{E}_\alpha \left\{ \min_{\rho>0} \Pi_{(i,l)\in\mathcal{E}} \mathbb{E}_{Y_{i,l}|\alpha} \left[e^{-\rho Y_{i,l}} \middle| \, d_i, j \right] \right\} \quad (19)$$

$$= \Pi_{(i,l)\in\mathcal{E}} \mathbb{E}_{\alpha_{l,\nu(i,k)}} \left\{ e^{-\frac{P^s \alpha_{l,\nu(i,k)}^2}{2\sigma_{\nu(i,k)}^2}} \right\} \quad (20)$$

$$= \Pi_{(i,l)\in\mathcal{J}} \left(\mathbb{E} \left\{ \Pi_{k=1}^{2R} \frac{exp\left(\frac{-\bar{\alpha}_D^2 P^s}{2\sigma_{l,\nu(i,k)}^2 + \bar{\alpha}_R^2 P^s} \right)}{1 + \bar{\alpha}_R^2 P^s / 2\sigma_{l,\nu(i,k)}^2} \right\} \right) \times \Pi_{(i,l)\in(\mathcal{E}-\mathcal{J})} \left\{ \Pi_{k=1}^{2R} \frac{exp\left(\frac{-\bar{\alpha}_D^2 P^s}{2\sigma_B^2 + \bar{\alpha}_R^2 P^s} \right)}{1 + \bar{\alpha}_R^2 P^s / 2\sigma_B^2} \right\} \quad (21)$$

$$= \left\{ \sum_{k=N_{min}}^{N_{max}} G_{k,N_J} \left(\frac{exp\left(\frac{-\bar{\alpha}_D^2 P^s}{2\sigma_J^2+\bar{\alpha}_R^2 P^s}\right)}{1+\bar{\alpha}_R^2 P^s/2\sigma_J^2} \right)^k \left(\frac{exp\left(\frac{-\bar{\alpha}_D^2 P^s}{2\sigma_B^2+\bar{\alpha}_R^2 P^s}\right)}{1+\bar{\alpha}_R^2 P^s/2\sigma_B^2} \right)^{2R-k} \right\}^j \left\{ \left(\frac{exp\left(\frac{-\bar{\alpha}_D^2 P^s}{2\sigma_B^2+\bar{\alpha}_R^2 P^s}\right)}{1+\bar{\alpha}_R^2 P^s/2\sigma_B^2} \right)^{2R} \right\}^{d_i-j}, \quad (22)$$

where $\alpha = \{\alpha_{l,\nu(i,k)}\}_{(i,l)\in\mathcal{E}}$ is a set of channel gains, $\sigma_B^2 = Var[I_q^{\nu(i,k)}[l]] + \sigma_0^2$, and $N_J = \rho_F N$ is the number of subcarriers being jammed. In (22), $N_{min} = \max\{2R - (N - N_J), 0\}$ and $N_{max} = \min\{N_J, 2R\}$ are, respectively, the minimum and maximum number of diversity components that are being jammed, given there are N_J out of N subcarriers that are jammed.

The inequality in (18) comes from the Chernoff bound. The interchange of operations in (19) is justified as follows. When conditioned on α and the $\{d_i\}$'s, the random variables $\{Y_{i,l}\}$ are jointly uncorrelated (hence independent) Gaussian random variables. So we have

$$\begin{aligned} &\mathbb{E}_{Y_{i,l}|\gamma}\left[e^{-\rho\left(\sum_{(i,l)\in\mathcal{E}} Y_{i,l}\right)} \Big| d_i, j \right] \\ &\quad = \mathbb{E}_{Y_{i,l}|\gamma}\left[\Pi_{(i,l)\in\mathcal{E}} e^{-\rho Y_{i,l}} \big| d_i, j \right] \\ &\quad = \prod_{(i,l)\in\mathcal{E}} \mathbb{E}_{Y_{i,l}|\gamma}\left[e^{-\rho Y_{i,l}} \big| d_i, j \right]. \end{aligned} \quad (23)$$

The calculation from (21) to (22) involves averaging over the partial-band jamming status. For a given value of ρ_F, the number of jammed subcarriers ranges from N_{min} to N_{max}, and the probability that k out of $2R$ diversity components are jammed for a given N_J is G_{k,N_J} when $N_{min} \le k \le N_{max}$, and zero otherwise. Note that this step is needed here because we only assume knowledge of the number of bands jammed and the weight enumeration function of the code used. If we have knowledge of which subcarriers are jammed and the structure of the encoder, then it is possible to track which coded symbols are affected and use the result presented in [2]. Since we have eliminated both assumptions, an extra averaging step is needed to obtain the averaged performance.

Finally, using the input-output enumeration function of the convolutional code, the union bound on the bit error probability is

$$P_b \le \sum_{d_i=d_{free}}^{\infty} A(d_i) \overline{P\left(U^{(1)} - U^{(0)} \ge 0 \big| d_i\right)}, \quad (24)$$

where d_{free} is the free distance of the code, and $A(d_i)$ is the number of different codewords that are at distance d_i from the $r = 0$ path.

B. Hard Decision Decoding

In the previous subsection, the diversity components from each subcarrier are assumed to be maximal-ratio combined. The coefficients as described in (8) require not only channel state information (CSI) α, but also jammer state information (JSI) σ_J. In this section, we assume the majority voting combining, described in Section II-C.2, is used. Note that neither CSI nor JSI is required for this combining scheme. Because we have established at the beginning of Section III-A that the partial-time jamming mode does not have an impact on the average performance when the jammer has no information of system interleaver structure, only the individual jamming mode is considered here. Similar to the analysis in Section III-A, assume the all-zero sequence was sent. Then Y_l is a vector of $0's$ and $1's$ and is the input to the hard-decision Viterbi decoder. Let

$$P(d_i) \triangleq Pr(U^{(1)} \ne U^{(0)} | \mathbf{Y}, \alpha, jammer), \quad (25)$$

where $U^{(1)}$ is the code path that the decoder has chosen, $\mathbf{Y}$ consists of the decisions of the channel output, and $U^{(0)}$ is the all-zero path. The Hamming distance between $U^{(0)}$ and $U^{(1)}$ is d_i. Then we can upper bound the error probability with the union bound in (24).

Let $\hat{\mathbf{x}}$ and $\mathbf{x}$ be the code sequences associated with paths $U^{(1)}$, and $U^{(0)}$, respectively. We can bound $P(d_i)$ by modifying the Chernoff bound for hard-decision decoding given in [10]:

$$P(d_i) = Pr\{\sum_{i\in\mathcal{E}} [\mu(Y_i', \hat{x}_i) - \mu(Y_i', x_i)] \ge 0 | \mathbf{x}, \alpha\} \quad (26)$$

$$\le \Pi_{i\in\mathcal{E}} \sqrt{4p_i(1-p_i)}, \quad (27)$$

where $Y_i, x_i, \hat{x}_i$ are elements in sequences $\mathbf{Y}, \mathbf{x}, \hat{\mathbf{x}}$ respectively, $\mathcal{E}$ is the set of indices where $\mathbf{x} \ne \hat{\mathbf{x}}$, and the cardinality of $\mathcal{E}$ is d_i. Finally, $\mu(Y_i, x_i)$ is the Hamming distance between Y_i and x_i, where p_i is the crossover probability for the ith symbol. Note that p_i is determined by both the instantaneous channel gain and the state of the jammer.

We now average (27) over the jammer state and the channel, analogous to the soft-decision decoding case and obtain

$$\overline{P(d_i)} = \sum_{j=0}^{d_i} \binom{d_i}{j} \rho_T^j (1-\rho_T)^{d_i-j} \left(\mathbb{E}_\alpha\left\{\sqrt{4p_o(1-p_o)}\right\}\right)^{(d_i-j)} \left(\sum_{k=N_{min}}^{N_{max}} \frac{\binom{N_J}{k}\binom{N-N_J}{2R-k}}{\binom{N}{2R}} D_{i,k} \right)^j, \quad (28)$$

where $D_{i,k}$ is defined as

$$D_{i,k} \triangleq \mathbb{E}_\alpha\left\{\sqrt{4p_{i,k}(1-p_{i,k})}\right\}, \quad (29)$$

and $p_{i,k}$ is the probability of error when k out of the $2R$ components are jammed.

Let $p_{i,k}^j$ be the probability that k out of $2R$ components are jammed and j out of $2R$ copies voted for the wrong decision. Then $p_{i,k}$ can be calculated as

$$p_{i,k} = \sum_{j=R+1}^{2R} p_{i,k}^j + \frac{1}{2} p_{i,k}^R. \quad (30)$$

To calculate $p_{i,k}^j$, define $p_{i,k}^{j,l}$ as the probability that k out of $2R$ components are jammed, j out of $2R$ copies voted for the wrong decision, and l of the copies that voted for the

wrong decision are affected by the jammer. Then $p_{i,k}^{j,l}$ has the following expression:

$$p_{i,k}^{j,l} = \Pi_{m=1}^{l}\left[Q\left(\frac{\sqrt{P^s}\alpha_{\nu(i,m)}}{\sigma_J}\right)\right] \Pi_{m=l+1}^{k}\left[1-Q\left(\frac{\sqrt{P^s}\alpha_{\nu(i,m)}}{\sigma_J}\right)\right] \Pi_{m=k+1}^{j-l+k}\left[Q\left(\frac{\sqrt{P^s}\alpha_{\nu(i,m)}}{\sigma_B}\right)\right] \Pi_{m=k+j-l+1}^{2R}\left[1-Q\left(\frac{\sqrt{P^s}\alpha_{\nu(i,m)}}{\sigma_B}\right)\right]. \quad (31)$$

Note that for given values of j, k, and $2R$, we can see that the maximum value l can take is $l_{max} = \min\{j, k\}$, and the minimum value l can take is $l_{min} = \max\{j-(2R-k), 0\}$, where l_{max} is obtained by considering k copies are affected by the jammer and j copies voted for the wrong decision. So the total number of jammed copies that voted for the wrong decision must be less than the smaller value of j and k. Similarly, l_{min} is obtained by noting $2R-k$ is the number of copies not affected by the jammer. As a result, when $j \geq 2R-k$, $j-(2R-k)$ is the minimum number of error copies that will always be affected by the jammer, and the minimum number of error copies affected by the jammer cannot be less than zero.

Finally, $p_{i,k}^{j}$ equals

$$p_{i,k}^{j} = \sum_{l=l_{min}}^{l_{max}} \binom{k}{l}\binom{2R-k}{j-l} p_{i,k}^{j,l}. \quad (32)$$

Using (31), (32), (30), (29), (28), and (24), the performance of the system with majority voting and hard-decision decoding can be bounded.

IV. Jamming Parameter Selection

From the above analysis, although the performance bound for hard-decision decoding relies on numerical evaluation to estimate the performance, the bound for soft-decision decoding allows for faster jamming parameter selection. In this section, we look into the optimization for a Rician fading environment based on the bound, with Rayleigh fading as a special case.

A. General Rician Fading

Let

$$g_{N_J}(\rho_T) \triangleq \sum_{k=N_{min}}^{N_{max}}\left[G_{k,N_J}\left(\frac{exp\left(\frac{-\bar{\alpha}_D^2 P^s}{2\sigma_J^2+\bar{\alpha}_R^2 P^s}\right)}{1+\bar{\alpha}_R^2 P^s/2\sigma_J^2}\right)^k \left(\frac{exp\left(\frac{-\bar{\alpha}_D^2 P^s}{2\sigma_B^2+\bar{\alpha}_R^2 P^s}\right)}{1+\bar{\alpha}_R^2 P^s/2\sigma_B^2}\right)^{2R-k}\right]. \quad (33)$$

In $g_{N_J}(\rho_T)$, the last component is a constant that does not depend on the jamming parameters, and σ_J^2 is shorthand for $\sigma_J^2(\rho_T)$. Note that for fixed ρ_F, σ_J^2 is only a function of ρ_T and can be written as

$$\sigma_J^2 = \sigma_B^2 + \frac{\eta_{J_F}}{2\rho_T N_c} \quad (34)$$

for $0 < \rho_T \leq 1$. $\eta_{J_F} \triangleq \eta_{J_0}/\rho_F$ is a constant for fixed ρ_F/N_J.

Plugging (22) and (33) into (15), we obtain

$$P(U^{(1)}-U^{(0)} \geq 0|d_i) \leq \sum_{j=0}^{d_i}\binom{d_i}{j}[\rho_T g_{N_J}(\rho_T)]^j \left[(1-\rho_T)\left(\frac{exp\left(\frac{-\bar{\alpha}_D^2 P^s}{2\sigma_B^2+\bar{\alpha}_R^2 P^s}\right)}{1+\bar{\alpha}_R^2 P^s/2\sigma_B^2}\right)^{2R}\right]^{d_i-j} \quad (35)$$

$$= \left[\rho_T g_{N_J}(\rho_T) + (1-\rho_T)\left(\frac{exp\left(\frac{-\bar{\alpha}_D^2 P^s}{2\sigma_B^2+\bar{\alpha}_R^2 P^s}\right)}{1+\bar{\alpha}_R^2 P^s/2\sigma_B^2}\right)^{2R}\right]^{d_i}. \quad (36)$$

Because $g_{N_J} > 0$, we have

$$0 < \rho_T g_{N_J}(\rho_T) + (1-\rho_T)\left(\frac{exp\left(\frac{-\bar{\alpha}_D^2 P^s}{2\sigma_B^2+\bar{\alpha}_R^2 P^s}\right)}{1+\bar{\alpha}_R^2 P^s/2\sigma_B^2}\right)^{2R}. \quad (37)$$

Since d_i is a positive integer by definition, we can conclude that, given the value of N_J, the value of ρ_T that maximizes the bound for $P(U^{(1)}-U^{(0)} \geq 0|d_i)$ is the same ρ_T that maximizes the function $h_{N_J}(\rho_T)$ defined in (38), which is independent of the value d_i:

$$h_{N_J}(\rho_T) \triangleq \rho_T g_{N_J}(\rho_T) + (1-\rho_T)\left(\frac{exp\left(\frac{-\bar{\alpha}_D^2 P^s}{2\sigma_B^2+\bar{\alpha}_R^2 P^s}\right)}{1+\bar{\alpha}_R^2 P^s/2\sigma_B^2}\right)^{2R}. \quad (38)$$

Furthermore, from (24), it can be seen that the average error rate bound of the code is a linear combination, with positive coefficients, of $P(U^{(1)}-U^{(0)} \geq 0|d_i)$. We conclude that the ρ_T that maximizes $h_{N_J}(\rho_T)$ also maximizes the error rate bound of the system, for a fixed value of N_J. To find the optimal ρ_T based on the bound, we calculate the first derivative of $h_{N_J}(\rho_T)$

$$h'_{N_J}(\rho_T) = g_{N_J}(\rho_T) + \rho_T g'_{N_J}(\rho_T) - T_1, \quad (39)$$

where $g'_{N_J}(\rho_T)$ is given by

$$g'_{N_J}(\rho_T) = \sum_{k=N_{min}}^{N_{max}} C_k \left[k\left(\frac{exp\left(\frac{-\bar{\alpha}_D^2 P^s}{2\sigma_J^2+\bar{\alpha}_R^2 P^s}\right)}{1+\bar{\alpha}_R^2 P^s/2\sigma_J^2}\right)^{k-1} \frac{exp\left(\frac{\bar{\alpha}_D^2 P^s}{\eta_{J_F}/(N_c\rho_T)+\bar{\alpha}_R^2 P^s}\right)}{\left(1+\frac{2\bar{\alpha}_R^2 N_c P^s}{\eta_{J_F}}\rho_T\right)^2} \times \frac{\left(\bar{\alpha}_D^2 P^s \frac{\eta_{J_F}}{N_c}\right)\left(1+\frac{2\bar{\alpha}_R^2 N_c P^s}{\eta_{J_F}}\rho_T\right) - \frac{2\bar{\alpha}_R^2 N_c P^s}{\eta_{J_F}}}{\left(\frac{\eta_{J_F}}{N_c}+\bar{\alpha}_R^2 P^s \rho_T\right)^2}\right], \quad (40)$$

and

$$T_1 = \left(\frac{exp\left(\frac{-\bar{\alpha}_D^2 P^s}{2\sigma_B^2 + \bar{\alpha}_R^2 P^s}\right)}{1 + \bar{\alpha}_R^2 P^s / 2\sigma_B^2} \right)^{2R},$$

$$C_k = G_{k,N_J} \left(\frac{exp\left(\frac{-\bar{\alpha}_D^2 P^s}{2\sigma_B^2 + \bar{\alpha}_R^2 P^s}\right)}{1 + \bar{\alpha}_R^2 P^s / 2\sigma_B^2} \right)^{2R-k}.$$

The roots of $h'_{N_J}(\rho_T) = 0$ can be found numerically, and through comparison, we can determine the optimal ρ_T for a fixed N_J based on the bound. Those values are not guaranteed to be the global optimal point, since the analysis is not based on the true error rate expression.

B. Rayleigh Fading

When Rayleigh fading is considered, the K-factor equals 0. This results in $\bar{\alpha}_D^2 = 0$ and $\bar{\alpha}_R^2 = \bar{\alpha}_q^2$, and $h_{N_J}(\rho_T)$ and the first derivative of $h_{N_J}(\rho_T)$ become

$$h_{N_J}(\rho_T) = \rho_T g_{N_J}(\rho_T) + (1 - \rho_T) \left(\frac{1}{1 + \bar{\gamma}_o} \right)^{2R}, \tag{41}$$

$$h'_{N_J}(\rho_T) = \sum_{k=N_{min}}^{N_{max}} C_k^{(2)} \left[\left(\frac{1}{1 + \bar{\gamma}_J(\rho_T)} \right)^k - k\bar{\gamma}_J(\rho_T) \left(1 - \frac{\bar{\gamma}_J(\rho_T)}{\bar{\gamma}_o} \right) \left(\frac{1}{1 + \bar{\gamma}_J(\rho_T)} \right)^{k+1} \right] - T_2. \tag{42}$$

where

$$T_2 = (1/(1 + \bar{\gamma}_o))^{2R},$$
$$C_k^{(2)} = G_{k,N_J} \left(1/(1 + \bar{\gamma}_o)\right)^{2R-k}.$$

Note that $\bar{\gamma}_o$ is a constant that does not depend on ρ_T, ρ_F. For a fixed N_J, $\bar{\gamma}_J(\rho_T)$ is a function of ρ_T. Setting $h'_{N_J}(\rho_T) = 0$, and multiplying both sides by $(1 + \bar{\gamma}_J)^{N_{max}+1}$ we have

$$\sum_{k=N_{min}}^{N_{max}} C_k^{(2)} \left[(1 + \bar{\gamma}_J(\rho_T))^{N_{max}+1-k} - k\bar{\gamma}_J(\rho_T) \left(1 - \frac{\bar{\gamma}_J(\rho_T)}{\bar{\gamma}_o} \right) (1 + \bar{\gamma}_J(\rho_T))^{N_{max}-k} \right] = T_2 \left(1 + \bar{\gamma}_J(\rho_T)\right)^{N_{max}+1}. \tag{43}$$

In general, the above equation has at most $\max\{N_{max} + 1, N_{max} - N_{min} + 2\}$ positive real roots (Descartes' Rule). Since $N_{max} \leq 2R$, $N_{min} \geq 0$, there are at most $2R + 2$ positive real roots. To find, using the bound, the optimal value of ρ_T for a given ρ_F or N_J, we have to compare at most $2R+4$ (including 0 and 1) points. So the number of comparisons needed to find the optimal pair (ρ_T, N_J) is at most $N(2R+4)$.

V. Numerical Results

In this section, results based on both simulation and numerical calculations are presented and discussed. Throughout the simulation, we use maximal-length PN sequences. In order to compare our results with results in existing literature, Rayleigh fading channels are used for the first set of results. We also define JSR to be

$$JSR \triangleq \frac{jamming\ power}{signal\ power} = \frac{\eta_{J_0}(MRN_{bits})W}{E_b/T_b}. \tag{44}$$

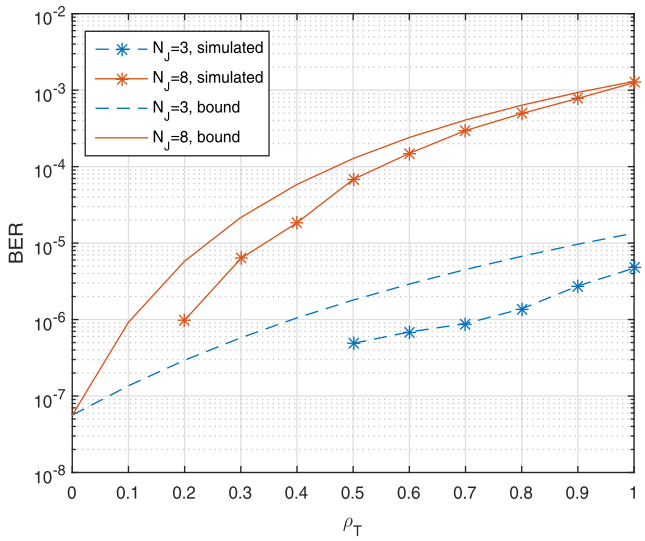

Fig. 3. BER performance with partial-time, partial-band jamming in Rician fading. E_b/η_o=10dB, JSR=30dB, 10 users, M = 4, R = 2, N_{bits} = 1, N = 8, $K_{fac} = 5$.

A. Individual Symbol Jamming

Fig. 3 compares simulated partial-time, partial-band jamming with the analytical results derived in this paper. In the simulation, a rate–1/4 convolutional code with generating polynomial [25,27,33,37] (in octal) was used. The channel is assumed to experience Rician fading with K-factor equal to 5, the frequency diversity parameter $R = 2$ was chosen, E_b/η_o was set to be 10dB, and JSR = 30dB. The total number of subcarriers in the system is $N = 8$. For each simulated point, either a minimum of 5,000 errors was collected, or 500 rounds of simulation were performed, depending on which condition was satisfied first. Simulated and analytical results for partial-band jamming with $N_J = 3$, and full-band jamming with $N_J = 8$, are plotted. We can see that the analytical result is an upper bound to the simulated performance.

B. Burst Jammer With Random Interleaver

Fig. 4 compares the simulated average error probability for individual symbol jamming and burst jamming within a codeword with the derived bound given in Section III-A. For this simulation, each user has fixed $E_b/\eta_o = 20$dB per user. The number of users in the system is 10, $N_c = 16$, and a length-1023 pseudo-random sequence is used. The convolutional code used in this simulation is a rate–$1/3$ code with generating polynomial given by [25,33,37] in octal. The theoretical result was modified such that whenever the calculated bound for P_b is greater than 1, it is set to 1. Each point results from an average of 50,000 bits. The points marked by a star were generated using a randomly selected interleaver and a block

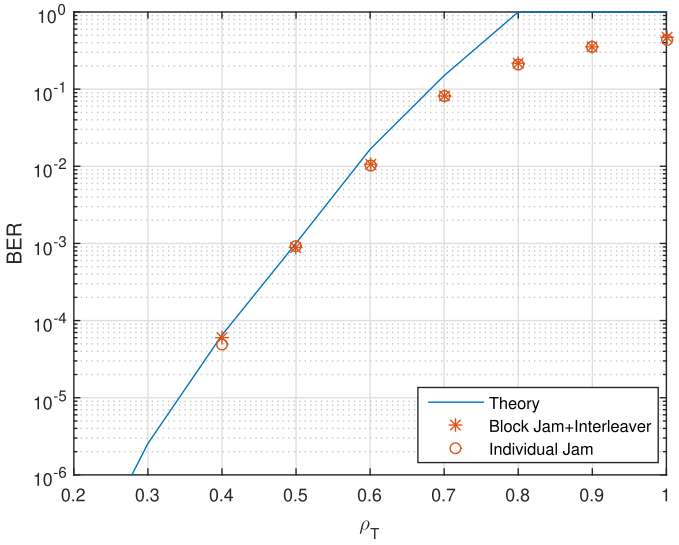

Fig. 4. Block jamming and individual symbol jamming BER performance comparison with partial-time jamming and FEC coding in Rayleigh fading. $E_b/\eta_o = 20$dB, JSR = 10dB, 10 users, M = 3, R = 3, $N_{bits} = 1$, N = 9.

jammer. For each realization, a different interleaver is selected at random and a different starting point was generated for the jammer. A total of 50 interleavers were tested. The points marked by circles were generated when each coded symbol is jammed with probability equal to ρ_T.

From the simulation result, it can be seen that when the interleaver structure is not known, the average performance of a block jammer with a randomly selected interleaver is comparable to the average performance of individual symbol jamming. As a result, the result derived based on the individual jamming model can be used as an upper bound on the average performance.

C. Jamming Strategy Comparison

In this section, we compare the effect of different jamming strategies on the system using the analytical results derived in this paper, and use the analytical bound to find the best jamming strategy for systems with different designs and in different environments.

1) Theoretical Result and Simulation Result Comparison: Fig. 5 compares the optimal jamming parameters selected based on the bound and based on simulation. To generate this plot, the K-factor of the channel is set to 10, and the system uses a rate–1/2 convolutional code, with a repetition order $2R = 4$, and uses hard-decision decoding with majority voting combining. For each tested JSR value, the simulation is performed for ρ_T values from 0 to 1 at a 0.05 step size. For each ρ_T value, N_J values from 1 to N are simulated. For each pair of jamming (ρ_T, N_J) values, either a minimum of 100 errors was collected, or 500 rounds of simulation were performed, depending on which condition was satisfied first. In both sub-figures, blue represents bound-indicated results and red represents simulation-indicated results.

Fig. 5a shows a gap exists between the optimal jamming parameters suggested by the bound and those based on actual simulation. This is inevitable since the bound we derived is an upper bound and is not based on full knowledge of the system construction. Fig. 5b shows the corresponding simulated BER values for the parameter set indicated by Fig. 5a at each JSR. The log-scale BER difference resulting from the jamming parameters suggested by the bound and those suggested by the simulation decreases as the jamming power increases. From the figures, we conclude the bound can accurately predict the optimal ρ_F parameter and is more accurate at predicting the partial-time jamming parameter at higher JSR values than at lower JSR values.

To examine the sensitivity of the bound-based optimal jamming strategy towards channel and system information mismatch, we compared optimal jamming parameters that were obtained by simulation with those obtained by the bounds derived in Section III, for cases where the jammer employs in the bound either correct or incorrect information regarding the system's E_b/η_o and the channel's K_{fac}.

For the soft-decision decoding system with maximal-ratio combining, we simulated jamming performance for a system with $JSR = 40$dB, $M = 2$, $R = 4$, $E_b/\eta_o = 12$dB in a Rayleigh fading channel, and found the jamming parameter pair $(\rho_T,\rho_F) = (1, 1)$ results in the largest BER. This is the simulated optimal jamming parameter pair, which is compared with the optimal jamming parameter pairs obtained by the jammer parameter optimization algorithm using the bound, with mismatched E_b/η_o and K_{fac} values used in the calculation. When given the correct $E_b/\eta_o = 12$dB and $K_{fac} = 0$ values, the algorithm produces $(\rho_T,\rho_F) = (1, 1)$ as the bound-based optimal pair, matching the simulation-based optimal pair. The algorithm is robust under both E_b/η_o value mismatch and K_{fac} mismatch. Keeping the K_{fac} input set to 0, we tested various mismatched E_b/η_o values ranging from 5dB to 100dB, and the bound-generated optimal jamming parameter pairs continued to be $(\rho_T,\rho_F) = (1, 1)$, agreeing with the simulated optimal pair. Keeping the E_b/η_o input to the algorithm at 12dB and examining K_{fac} mismatch, the bound-generated optimal parameter pair continued to be $(\rho_T,\rho_F) = (1, 1)$ through $K_{fac} = 100$, although at the extreme case where the input K_{fac} value to the jammer's optimization algorithm is taken to be 1000 while the true channel $K_{fac} = 0$, the bound-generated optimal parameter pair was $(\rho_T,\rho_F) = (0.164, 1)$, departing substantially from the optimal pair derived by simulation. From this we conclude that the bound is robust over a wide range of values under these system and channel conditions.

For the hard-decision decoding system with majority-voting combining, we obtained (through simulation) the optimal jamming parameter pair $(\rho_T,\rho_F) = (0.75, 1)$ for a system with $JSR = 10$dB, $M = 2$, $R = 2$, and $E_b/\eta_o = 15$dB, in a Rician fading channel with $K_{fac} = 10$. When compared to the bound-based optimal jamming parameter pairs with the correct $E_b/\eta_o = 15$dB and $K_{fac} = 10$ values, the bound-based optimal pair is $(\rho_T,\rho_F) = (1, 1)$. So there is a gap even with perfectly matched information at the jammer, as is shown in Fig. 5b. Keeping the E_b/η_o input at 15dB, as the K_{fac} input to the jammer's optimization algorithm varies, the bound-based optimal parameter pair does not vary even when the K_{fac} input value equals 1000. However, the bound-based

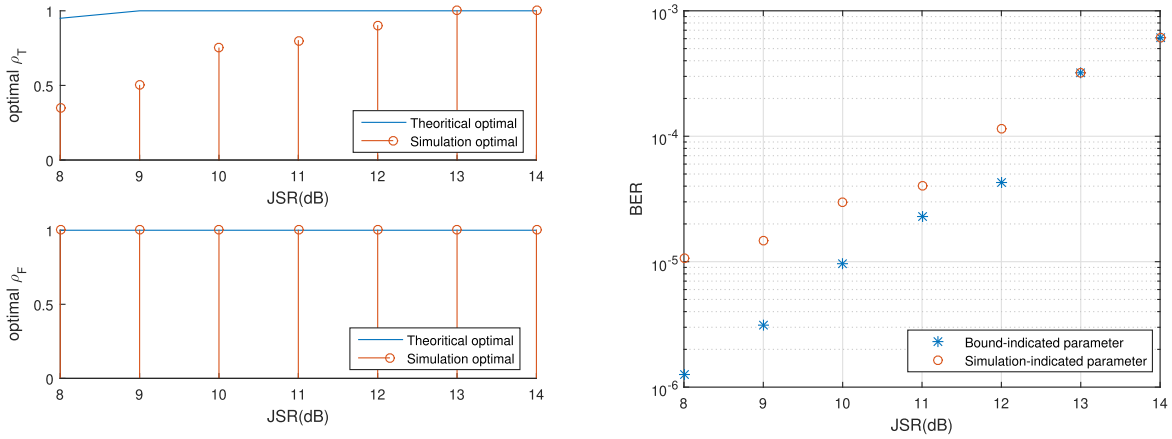

(a) Optimal jamming parameter selection

(b) Simulated BER comparison

Fig. 5. Bound-indicated optimal parameter and simulation-indicated optimal parameter comparison. Rician fading, $K_{fac} = 10$, $E_b/\eta_o = 15$dB, $M = 2$, $R = 2$, $N_{bits} = 1$, majority voting combining with hard-decision decoding.

optimal parameter pair is sensitive to the E_b/η_o input value. Keeping the K_{fac} input set to 10, as the input E_b/η_o value increases from the simulation setting of $E_b/\eta_o = 15$dB, the bound-based optimal ρ_F remains equal to 1 (matching the simulation optimal value) and the ρ_T parameter eventually decreases from 1, equaling 0.9, 0.85, and 0.7 at E_b/η_o values of 19dB, 20dB, and 50dB, respectively. We conclude that mismatch effects are fairly small.

2) Soft-Decision Decoding: Fig. 6 compares the effect of joint partial-time, partial-band jamming on MC-DS-CDMA systems with different parameters. In this figure, the system uses soft-decision decoding, the E_b/η_o value is 12dB, the JSR value is set to 20dB, $N_{bits} = 4$, and a rate–1/2 convolutional code was used. The plot shows the optimal ρ_T and ρ_F values as indicated by the bound, for varying channel K-factors. The parameters for this optimal point are found using the method described in Section IV. The blue curves correspond to when no frequency repetition is used by the system ($2R = 1$), and the red curves correspond to when a frequency repetition order of 2 is used. Also, $N = 4$ for the first system, and $N = 8$ for the second system. The spreading factors of the systems are chosen to guarantee the total system bandwidth and data rate stay the same.

When no frequency repetition is used, full-time, full-band jamming appears to be (based upon our numerical results) optimal at low K-factor values. As the channel's line-of-sight component becomes stronger, joint partial-time, partial-band jamming starts to cause the most damage to the system. When frequency repetition is present in the system, full-band jamming causes more damage than partial-band jamming, and a jammer optimizing its parameters using the bound will switch from a full-time, full-band jamming strategy to a partial-time, full-band jamming strategy as the K-factor of the channel increases. This result is consistent with research on fast frequency-hopped spread-spectrum systems, such as [12] and [16], and is consistent with results in [8], where frequency repetition is always used.

This result is caused by our system model. Based on our model, all copies of any coded-symbol are transmitted during the same symbol duration and repeated across one or more subcarriers. When copies of the same symbol are transmitted on two or more subcarriers, partial-band jamming cannot guarantee all copies are jammed. When maximal-ratio combining with optimal coefficients is used, the deeply-faded or heavily-jammed copies contribute little to the final coded-symbol statistics. Thus, the impact of partial-band jamming on the system error rate is small. On the other hand, a partial-time, full-band jammer will guarantee all the coded-symbols transmitted during the jammed time slots are completely affected by the jammer; this can affect the jammed coded-symbol error rate significantly, resulting in a higher decoded error rate.

The frequency repetition here can be viewed as an additional layer of coding across subcarriers. By using frequency repetition, we are exploiting frequency diversity in fading channels and also using a lower rate code, hence more protection, across subcarriers. The results we obtained here suggest that when more protection is given to the time or frequency dimension than the other, the jammer should jam a higher percentage of the more heavily protected dimension to guarantee a higher overall error rate.

The result that in the extreme case when Rayleigh fading is considered ($K_{fac} = 0$), full-time, full-band jamming is optimal regardless of system construction is consistent with previous literature. In [9, Vol.2, ch.1.6.4] the authors argued that a full-time jammer is optimal for a DS-CDMA system under Rayleigh fading because the fading has already created the same impact as that of a worst-case partial-time jammer, so the changes in the received signal-to-interference-and-noise-ratio introduced by a partial-time jammer no longer have a major impact on the performance of the system. A similar argument can be made here to support the result that full-time, full-band jamming is selected as optimal based on the bound for an MC-DS-CDMA system with maximal-ratio combining under Rayleigh fading.

3) Hard-Decision Decoding: Figs. 7 and 8 plot the optimal jamming parameters based on the bound for a system using hard-decision decoding. In both figures, the upper plot shows

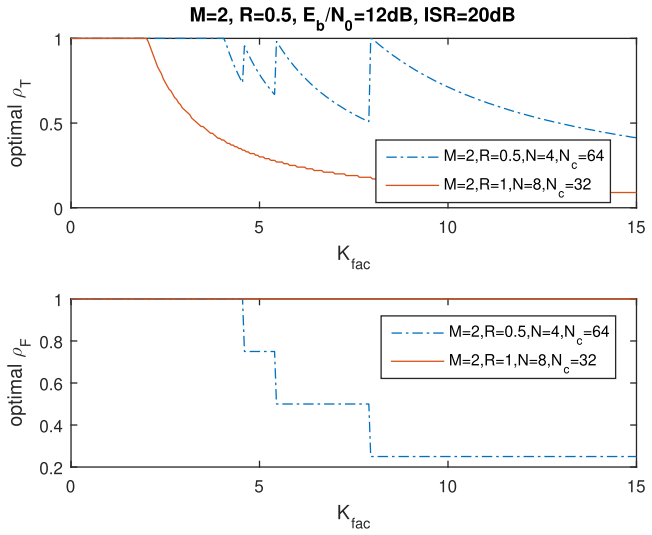

Fig. 6. Optimal jamming parameters selected based on the bound with maximal-ratio combining in different channel environment. $E_b/\eta_o = 12$dB, $JSR = 20$dB, $N_{bits} = 4$.

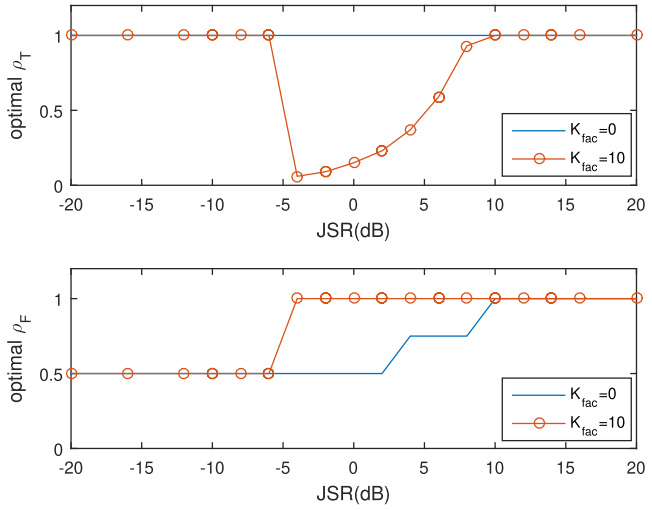

Fig. 7. Optimal jamming parameters selected based on the bound with majority combining in Rician fading. $E_b/\eta_o = 15$dB, M = 2, R = 2, $N_{bits} = 1$, N = 4.

the optimal ρ_T parameter and the lower plot shows the optimal ρ_F parameter, both based on the bound. The two values combined will define the optimized jamming strategy.

In Fig. 7, the system has $M = 2$, $2R = 4$, $N_{bits} = 1$, $N = 4$, and $E_b/\eta_o = 15$dB. Two K-factors are considered. Unlike the soft-decision decoding case, for both K-factors, partial-band jamming is best at lower JSR values. When $K_{fac} = 0$ (Rayleigh fading), an optimal jammer, as indicated by the bound, will choose to do full-time, partial-band jamming when the total jamming power is low, and transition to full-time, full-band jamming as the jamming power increases. For Rician fading with $K_{fac} = 10$, a jammer optimizing its parameters based on the bound will choose to do full-time, partial-band jamming when the total jamming power is low, and as more power is given to the jammer, partial-time jamming will become more beneficial than partial-band jamming and the jammer will switch from full-time, partial-band jamming to partial-time, full-band jamming. Ultimately the jammer switches to full-time, full-band jamming when the jamming power is large enough.

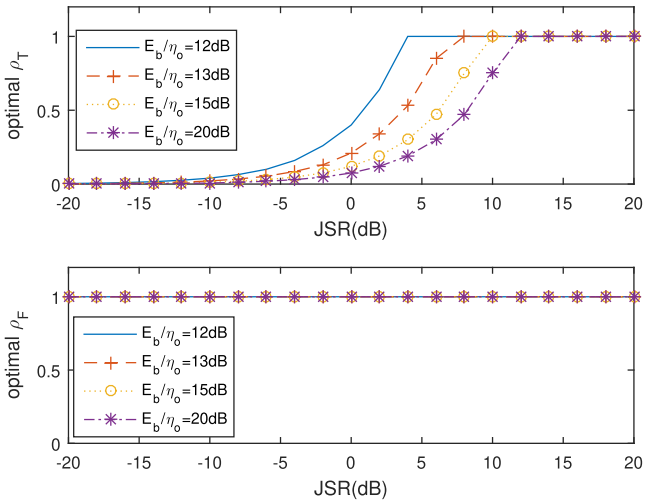

Fig. 8. Optimal jamming parameters selected based on the bound with majority combining in AWGN channel. M = 2, R = 2, $N_{bits} = 1$, N = 4.

Unlike the maximal-ratio combiner with optimal coefficients, which attenuates the deeply-faded/strongly-jammed components, the majority voting combiner makes a decision on each component independently without CSI and JSI, and requires at least half of the components to make a wrong decision to have the final decision be wrong. This means a partial-band jammer has a better chance to cause an FEC-coded symbol error when the majority-voting combiner is used than when the maximal-ratio combiner is used. As a result, we see full-time, partial-band jamming being indicated as optimal when the jamming power is low for the tested E_b/η_o value. Note that in this jamming power region, the full-time, partial-band jammer still cannot guarantee a FEC-coded symbol error on the jammed symbols. As jamming power increases, a partial-time, full-band jammer can result in a very high coded-symbol error rate for the jammed symbol for channels with a strong line-of-sight component, and the suggested optimal jamming strategy takes a complete switch from full-time, partial-band jamming to partial-time, full-band jamming. In this region, jammed symbols were observed to have significantly higher error rate compared to unjammed symbols; most of the jammed symbols have error rate at $0.3-0.5$. As the jamming power continues to increase, the suggested optimal jamming strategy will eventually become full-time, full-band.

Fig. 8 plots the optimal jamming parameters for the extreme case when $K_{fac} = \infty$ (AWGN channel) based on the bound. The system parameters are $M = 2$, $2R = 4$, $N_{bits} = 1$, and $N = 4$, and different values of E_b/η_o and JSR are considered. In this case, the suggested partial-band jamming parameter ρ_F is 1 for all values of E_b/η_o and JSR tested. As the jammer power JSR increases, the jammer switches from a partial-time, full-band jammer to a full-time, full-band jammer. The minimum JSR required for full-time, full-band

jamming to be optimal is monotonically decreasing in E_b/η_o. As E_b/η_o drops below 11dB, we observed full-time, full-band jamming to be optimal for all evaluated JSR values. Note that, while the optimal ρ_F is 1 for all the evaluated E_b/η_o values and JSR values in this system, we conjecture that in a system with more subcarriers and/or less protection in the frequency dimension, partial-band jamming is more likely to be optimal when the jamming power is limited. The results here are again consistent with [8].

VI. Conclusions

This paper extends the results of [8] by adding noise and error correction, and extends [2] by considering partial-time jamming in addition to partial-band jamming. It also extends the results in [8] and [2] to a more general Rician fading environment. Based on the two combining-decoding schemes, we have the following conclusions:

A. Soft-Decision Decoding With Maximal-Ratio Combining

With soft-decision decoding and maximal-ratio combining, our bound suggests that full-time, full-band jamming is most effective for all JSR values for a system in Rayleigh fading regardless of whether more protection is given to the subcarriers by the system. In a Rician fading environment with low JSR, if the system puts more protection across subcarriers than across time slots, partial-time, full-band jamming should be used; if the system puts equal amounts of protection across frequency and time, partial-time, partial-band jamming is more effective. As more jamming power is available to the jammer, the optimal jamming strategy will eventually switch to full-time, full-band jamming.

It can be concluded that when attacking a system using soft-decision decoding and maximal-ratio combining, full-time, full-band jamming is preferred when there is no line-of-sight component in the channel environment. With channels that have a line-of-sight component, the jammer should move in the direction of covering a higher percentage of the frequency/time dimension with more heavily protection than the dimension with lighter protection.

B. Hard-Decision Decoding With Majority Voting Combining

With hard-decision decoding and majority-voting combining, assuming Rician fading with $K_{fac} \neq 0, \infty$, full-time, partial-band jamming was shown, by our bound, to be more efficient in the low jamming power region at the evaluated system parameters. As jamming power increases, a jammer with optimized parameters based on the bound switches from full-time, partial-band jamming to partial-time, full-band jamming, and eventually to full-time, full-band. At the extreme case of $K_{fac} = 0$, the tested system shows that the optimized jammer based on the bound skips the partial-time, full-band jamming stage and transitions directly from full-time, partial-band to full-time, full-band as jamming power increases; for the other limiting case of $K_{fac} = \infty$, the suggested jamming strategy was shown to transition from partial-time, full-band to full-time, full-band. The fact that full-band jamming is optimal for the examined values of E_b/η_o and jamming power in an AWGN environment is consistent with previous literature.

From this result we conclude that, unlike the soft-decoding with maximal-ratio combining case, when attacking systems using hard-decision decoding and majority voting combining, partial-band jamming can cause more damage than full-band in a Rayleigh fading environment when the jamming power is low. With increasing available jamming power, we should switch from partial jamming to uniform jamming. When a line-of-sight component is present in the channel, full-time, partial-band jamming is preferred over the partial-time, full-band jamming (which covers more of the more heavily protected dimension) at low jamming power due to the effect of majority-voting combining. But with increasing jamming power we would still switch to a strategy covering a higher percentage of the more heavily protected dimension for the non-AWGN channel case. For the system considered corresponding to the AWGN channel case, the jammer should always jam a greater percentage of the more heavily protected dimension.

References

[1] D. N. Rowitch and L. B. Milstein, "Convolutionally coded multicarrier DS-CDMA systems in a multipath fading channel. I. Performance analysis," *IEEE Trans. Commun.*, vol. 47, no. 10, pp. 1570–1582, Oct. 1999.

[2] D. N. Rowitch and L. B. Milstein, "Convolutionally coded multicarrier DS-CDMA systems in a multipath fading channel. II. Narrow-band interference suppression," *IEEE Trans. Commun.*, vol. 47, no. 11, pp. 1729–1736, Nov. 1999.

[3] G. K. Kaleh, "Frequency-diversity spread-spectrum communication system to counter bandlimited Gaussian interference," *IEEE Trans. Commun.*, vol. 44, no. 7, pp. 886–893, Jul. 1996.

[4] L. Vandendorpe, "Multitone direct sequence CDMA system in an indoor wireless environment," in *Proc. IEEE 1st Symp. Commun. Veh. Technol.*, Oct. 1993, pp. 1–8.

[5] L. Vandendorpe, "Multitone spread spectrum multiple access communications system in a multipath Rician fading channel," in *Proc. Int. Conf. Commun.*, May 1994, pp. 1638–1642.

[6] S. Hara and R. Prasad, "Overview of multicarrier CDMA," *IEEE Commun. Mag.*, vol. 35, no. 12, pp. 126–133, Dec. 1997.

[7] A. S. Ling and L. B. Milstein, "The effects of spatial diversity and imperfect channel estimation on wideband MC-DS-CDMA and MC-CDMA," *IEEE Trans. Commun.*, vol. 57, no. 10, pp. 2988–3000, Oct. 2009.

[8] K. Cheun, K. Choi, H. Lim, and K. Lee, "Antijamming performance of a multicarrier direct-sequence spread-spectrum system," *IEEE Trans. Commun.*, vol. 47, no. 12, pp. 1781–1784, Dec. 1999.

[9] M. K. Simon, J. K. Omura, R. A. Scholtz, and B. K. Levitt, *Spread Spectrum Communications Handbook*. New York, NY, USA: McGraw-Hill, 2002.

[10] J. G. Proakis and M. Salehi, *Digital Communications*. 5th ed., New York, NY, USA: McGraw-Hill, 2008.

[11] M. Soysa, P. C. Cosman, and L. B. Milstein, "Optimized spoofing and jamming a cognitive radio," *IEEE Trans. Commun.*, vol. 62, no. 8, pp. 2681–2695, Aug. 2014.

[12] J. J. Kang and K. C. Teh, "Performance of coherent fast frequency-hopped spread-spectrum receivers with partial-band noise jamming and AWGN," *IEE Proc.-Commun.*, vol. 152, no. 5, pp. 679–685, Oct. 2005.

[13] B. R. Vojcic and R. L. Pickholtz, "Performance of direct sequence spread spectrum in a fading dispersive channel with jamming," *IEEE J. Sel. Areas Commun.*, vol. 7, no. 4, pp. 561–568, May 1989.

[14] B. R. Vojcic and R. L. Pickholtz, "Performance of coded direct sequence spread spectrum in a fading dispersive channel with pulsed jamming," *IEEE J. Sel. Areas Commun.*, vol. 8, no. 5, pp. 934–942, Jun. 1990.

[15] C. S. Patel, G. L. Stuber, and T. G. Pratt, "Analysis of OFDM/MC-CDMA under channel estimation and jamming," in *Proc. IEEE Wireless Commun. Netw. Conf.*, Mar. 2004, pp. 954–958.

[16] R. Nikjah and N. C. Beaulieu, "Antijamming capacity and performance analysis of multiple access spread spectrum systems in AWGN and fading environments," in *Proc. IEEE ICC*, Jun. 2006, pp. 5153–5159.
[17] A. E. El-Mahdy, "Partial band jamming of multicarrier frequency hopping/binary phase shift keying receiver over a Rayleigh fading channel with imperfect channel estimation," *IET Commun.*, vol. 4, no. 3, pp. 285–294, Feb. 2010.
[18] D. J. Thuente and M. Acharya, "Intelligent jamming in wireless networks with applications to 802.11b and other networks," in *Proc. MILCOM*, Oct. 2006, pp. 1075–1081.
[19] Q. Peng, P. C. Cosman, and L. B. Milstein, "Spoofing or jamming: Performance analysis of a tactical cognitive radio adversary," *IEEE J. Sel. Areas Commun.*, vol. 29, no. 4, pp. 903–911, Apr. 2011.
[20] T. Song, K. Zhou, and T. Li, "CDMA system design and capacity analysis under disguised jamming," *IEEE Trans. Inf. Forensics Security*, vol. 11, no. 11, pp. 2487–2498, Nov. 2016.
[21] N. Tang, Y. Wang, Y.-X. Gou, and Y. Tian, "Performance analysis of a new kind of UWB signal," in *Proc. Int. Conf. Wireless Commun., Netw. Mobile Comput.*, Sep. 2007, pp. 542–545.
[22] M. K. Simon and M.-S. Alouini, "BER performance of multicarrier DS-CDMA systems over generalized fading channels," in *Proc. IEEE Commun. Theory Mini-Conf.*, Jun. 1999, pp. 72–77.
[23] Y.-H. Kim, I. Song, H. G. Kim, and J. Lee, "Design and performance analysis of a convolutionally coded overlapping multicarrier DS/CDMA system," *IEEE Trans. Veh. Technol.*, vol. 49, no. 5, pp. 1950–1967, Sep. 2000.
[24] J. Tan and G. L. Stuber, "Anti-jamming performance of multi-carrier spread spectrum with constant envelope," in *Proc. IEEE Int. Conf. Commun.*, May 2003, pp. 743–747.
[25] S. Kondo and L. B. Milstein, "Multicarrier CDMA system with cochannel interference cancellation," in *Proc. IEEE Veh. Technol. Conf.*, Jun. 1994, pp. 1640–1644.
[26] K. Wu, P. C. Cosman, and L. B. Milstein, "Joint partial-time partial-band jamming of a multicarrier DS-CDMA system in a fading environment," in *Proc. IEEE Global Conf. Signal Inf. Process. (GlobalSIP)*, Nov. 2018, pp. 1306–1310.

Kanke Wu received the B.S. degree in communication engineering from the Beijing Institute of Technology, Beijing, China, in 2013, and the M.S. degree in electrical engineering from the University of California at San Diego, San Diego, CA, USA, in 2016, where she is currently pursuing the Ph.D. degree. Her research interest is in wireless communications.

Pamela C. Cosman (S'88–M'93–SM'00–F'08) obtained her B.S. with Honor in Electrical Engineering from the California Institute of Technology in 1987, and her Ph.D. in Electrical Engineering from Stanford University in 1993. Following an NSF postdoctoral fellowship at Stanford and at the University of Minnesota (1993–1995), she joined the faculty of the Department of Electrical and Computer Engineering at the University of California, San Diego, where she is currently a Professor and holds the Dr. John and Felia Proakis Chancellor Faculty Fellowship.

Her research interests are in the areas of image and video compression and processing, and wireless communications. She has written over 250 technical papers in these fields, as well as one children's book, *The Secret Code Menace*, that introduces error correction coding through a fictional story. Dr. Cosman's awards include the ECE Departmental Graduate Teaching Award, Career Award from the National Science Foundation, Globecom 2008 Best Paper Award, HISB 2012 Best Poster Award, 2016 UC San Diego Affirmative Action and Diversity Award, 2017 Athena Pinnacle Award, and 2018 National Diversity Award from ECEDHA (Electrical and Computer Engineering Department Heads Association). Her administrative positions include serving as Director of the Center for Wireless Communications (2006–2008), ECE Department Vice Chair (2011–2014), and Associate Dean for Students (2013–2016).

Dr. Cosman has been a member of the Technical Program Committee or the Organizing Committee for numerous conferences, including most recently serving as Technical Program Co-Chair of ICME 2018. She was an associate editor of the IEEE COMMUNICATIONS LETTERS (1998–2001), and an associate editor of the IEEE SIGNAL PROCESSING LETTERS (2001–2005). She was the Editor-in-Chief (2006–2009) as well as a Senior Editor (2003–2005, 2010–2013) of the IEEE JOURNAL ON SELECTED AREAS IN COMMUNICATIONS. She is a member of Tau Beta Pi and Sigma Xi.

Laurence B. Milstein (S'66–M'68–SM'77–F'85) received the B.E.E. degree from the City College of New York, New York, NY, in 1964, and the M.S. and Ph.D. degrees in electrical engineering from the Polytechnic Institute of Brooklyn, Brooklyn, NY, in 1966 and 1968, respectively. From 1968 to 1974, he was with the Space and Communications Group of Hughes Aircraft Company, and from 1974 to 1976, he was a member of the Department of Electrical and Systems Engineering, Rensselaer Polytechnic Institute, Troy, NY. Since 1976, he has been with the Department of Electrical and Computer Engineering, University of California at San Diego, La Jolla, CA, where he is a Distinguished Professor, the holder of the Ericsson Chair in Wireless Communications Access Techniques, and a former Department Chairman, working in the area of digital communication theory with special emphasis on spread-spectrum communication systems. He has also been a consultant to both government and industry in the areas of radar and communications.

Prof. Milstein was an Associate Editor for Communication Theory for the IEEE TRANSACTIONS ON COMMUNICATIONS, an Associate Editor for Book Reviews for the IEEE TRANSACTIONS ON INFORMATION THEORY, an Associate Technical Editor for the *IEEE Communications Magazine*, and the Editor-in-Chief of the IEEE JOURNAL ON SELECTED AREAS IN COMMUNICATIONS. He has been a member of the board of governors of both the IEEE Communications Society and the IEEE Information Theory Society, and was the Vice President for Technical Affairs in 1990 and 1991 of the IEEE Communications Society. He was a former chair of the IEEE Fellows Selection Committee, and was a recipient of the 1998 Military Communications Conference Long Term Technical Achievement Award, an Academic Senate 1999 UCSD Distinguished Teaching Award, an IEEE Third Millennium Medal in 2000, the 2000 IEEE Communications Society Armstrong Technical Achievement Award, and various prize paper awards. He was also the recipient of the IEEE Communications Theory Technical Committee (CTTC) Service Award in 2009, the CTTC Achievement Award in 2012, and the 2015 UCSD Chancellor's Associates Award for Excellence in Graduate Teaching.